2021 18th International Conference on Electrical Engineering, Computing Science and Automatic Control (CCE). Mexico City, Mexico. November 10-12, 2021

DFT-based Phasor Estimator using a MAF with a Phase-lead Compensator

1st Rafael Escudero
School of Engineering and Sciences
Tecnologico de Monterrey
Mexico City, Mexico
0000-0002-4329-2002

2nd Luis Ibarra
School of Engineering and Sciences
Tecnologico de Monterrey
Mexico City, Mexico
0000-0002-7290-3001

3rd Pedro Ponce
School of Engineering and Sciences
Tecnologico de Monterrey
Mexico City, Mexico
0000-0001-7035-5286

4th Arturo Molina
School of Engineering and Sciences
Tecnologico de Monterrey
Mexico City, Mexico
0000-0001-5461-2879

***Abstract*—Due to the advancing complexity of the electric grid, phasor estimators are becoming essential for monitoring an electric grid, interacting as a *wireless sensor network*. Such a network comprises low-cost devices capable of running non-demanding algorithms; then, fast yet complex methods, e.g., *Kalman filters* and the *wavelet transform*, could not be implemented, and a more straightforward approach is needed. The *Fourier filter* (FF) is a standard solution since it has a low computational load and incorporates a *moving average filter* (MAF) that eliminates harmonics, however causing an undesirable phase delay. So then, it is proposed here to add a phase-lead compensator to the MAF to solve the phase delay problem while preserving the algorithm's simplicity. The resulting estimator was compared to the conventional FF and the *cosine filter* (CF) in IEEE C37.118.1 standardized tests including harmonic, amplitude, and phase angle step changes. The proposal met all the standard requirements, slightly increasing the estimation error, and was also tested over the IEEE 13 node test feeder, showing a faster response than the FF and the CF.**

***Index Terms*—Phasor estimation, Fourier filter, Moving average filter, Phase-lead compensator.**

I. Introduction

THE current electrical power system is a complex network moving toward even more complexity due to the diverse energy requirements that it has to address [1, p. 63]. As a result, it has become more vulnerable to faults, blackouts and usually lacks fault diagnostics [2]. Such issues arose an interest in developing a monitoring system to improve the electrical power system protection, which was first based on phasor measurement units, later leading to the wide-area synchrophasor measurement system concept [3]. However, wide-area synchrophasor measurement systems are costly—from 10 to 70 thousand US dollars per phasor measurement unit—and require wired communications installation and maintenance [2], [4]. As an alternative, wireless sensor networks offer some advantages like lower cost, rapid deployment, flexibility, and aggregated intelligence [2].

The wireless sensor network's main components are smart sensors, in charge of the phasor estimation process. However, smart sensors cannot manage high computational loads, demanding algorithms that fit their processing capacity [5] while meeting the IEEE Std C37.118.1. Such standard involves several tests such as variations in magnitude, phase, and appearance of harmonics [6]. Then, the phasor estimator running on a smart sensor must deal with such distortion, provide a fast response, and have a low computational load.

The methods used for phasor estimation can be divided into the ones based on the *discrete Fourier transform* (DFT) and those that are not. Among non-DFT-based techniques, one finds some based on the wavelet transform, Kalman filters, and phase-locked loops. These last have been complementary to improve the estimates of other methods, such as in [7], [8].

Concerning the wavelet transform-based phasor estimators, an iterative version that can estimate in a quarter cycle of the input signal—*recursive wavelet transform*—was proposed in [9]. It can be adapted to deal with harmonics but rising its already high computational load. Other recent proposals are the *improved recursive wavelet transform* [10] and the *empirical wavelet transform* [11], which showed good performances under dynamic tests, but the high computational load persists.

Kalman filters were used in [12] with a Taylor polynomial approximation of the dynamic phasor mathematical model, called by the authors Taylor-Kalman-Fourier filter, which produces a null phase delay and can be adapted to deal with harmonic components. However, such adaptation significantly increases the computational load. Later, a *double sub-optimal strong tracking Kalman filter* was proposed [13] where the *a priori* error covariance is calculated differently. It performed better than the Taylor-Kalman-Fourier filter but requiring even more computations.

On the other hand, DFT-based techniques are not as computationally demanding. These are the *Fourier filter* (FF) and the *cosine filter* (CF), which can deal with harmonics, have a lower computational load than that of the DFT and incorporate a *moving average filter* (MAF). The MAF excels in removing harmonics, has a simple digital realization, good effectiveness, and low computational burden [14]. However, it produces a significant phase delay, undesirable in applications like monitoring, protection, state estimation, and power system control. Solving the MAF's phase delay problem contributes to developing a phasor estimation algorithm capable of dealing with harmonics, exhibiting low computational load and faster transient response.

Therefore, this research proposes developing an FF-based phasor estimator with a phase-lead compensator to solve the phase delay problem. The compensator corresponds with the one introduced in [15], characterized by not degrading the MAF's harmonics attenuation. In Section II, the mathematical models of the FF, the CF, and the proposal's development are presented. In Section III, the tests to which the phasor estimator will be subjected are described. They include harmonics, amplitude jumps, phase angle jumps, and a simulated electrical fault case study. In Section IV, the results of each test are shown and, finally, in Section V, the conclusions are presented.

II. System development

The mathematical model of the FF is

$$X_1 = \frac{2}{N}\sum_{n=0}^{N-1} x(n)\left[\cos\left(\omega_1\, n\, T_s\right) - \mathrm{j}\sin\left(\omega_1\, n\, T_s\right)\right] \qquad (1)$$

whereas the mathematical model of the CF is

$$X_1 = \frac{2}{N}\sum_{n=0}^{N-1} \cos\left(\omega_1\, t_n\right)\left[x(n) - \mathrm{j}\, x\left(n - \frac{N}{4}\right)\right] \qquad (2)$$

where X_1 represents the estimated phasor at the fundamental frequency, $x(n)$ is the sample taken at the n-th time instant of the input signal, ω_1 is the fundamental signal's frequency, $T_s = 1/f_s$ is the sampling time and N is the total number of samples within the filter's window. Then, the input signal's amplitude $|X_1|$ and phase angle $\angle X_1$ can be computed with the following equations:

$$|X_1| = \sqrt{\mathrm{Re}\{X_1\}^2 + \mathrm{Im}\{X_1\}^2} \qquad (3)$$

$$\angle X_1 = \arctan\left(\frac{\mathrm{Im}\{X_1\}}{\mathrm{Re}\{X_1\}}\right). \qquad (4)$$

The N-samples averaging needed in (1) and (2) can be recursively computed by a MAF. The discrete transfer function of the MAF is:

$$G_{\mathrm{MAF}}(z) = \frac{1}{N}\,\frac{1 - z^{-N}}{1 - z^{-1}}. \qquad (5)$$

The MAF notches at frequencies $n\, f_c$ for all $n \in \mathbb{N}^+$, where $f_c = 1/(N\, T_s)$ is the MAF's cutoff frequency, and adds a 90° phase lag as can be seen in Fig. 1.

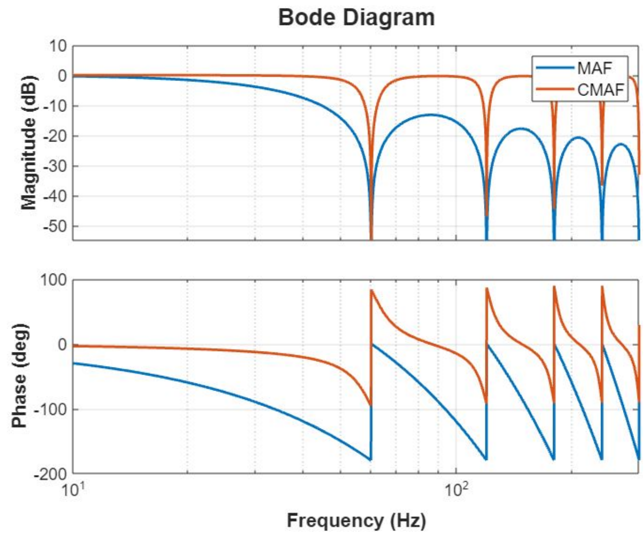

Fig. 1. Bode diagram of the MAF and the CMAF with $r = 0.95$.

Such lag can be reduced with a phase-lead compensator [15] whose transfer function is:

$$G_c(z) = k\,\frac{1 - r\, z^{-1}}{1 - r^N\, z^{-N}} \qquad (6)$$

where the *attenuation factor* $r \in [0, 1)$ and the gain k is defined by:

$$k = (1 - r^N)/(1 - r). \qquad (7)$$

When the MAF is cascaded with $G_c(z)$—forming the *phase-lead compensated moving average filter* (CMAF)—and r is selected close to unity, then the phase delay is compensated—see Fig. 1.

Up to this point, the phasor estimator could be implemented for integer values of N. However, having $N \in \mathbb{R}^+$ due to a non-integer $N = 1/f_c/T_s$ would impede implementation. Usually, N is rounded to the nearest integer, leading to numeric errors and estimation ripple. Therefore, the *weighted mean value* approach is used [14]:

$$G_{\mathrm{WCMAF}}(z) = (1 - \alpha)G_{\mathrm{CMAF}_f}(z) + \alpha\, G_{\mathrm{CMAF}_c}(z). \qquad (8)$$

This approach consists of the simultaneous action of two CMAFs, $G_{\mathrm{CMAF}_c}(z)$ uses the rounded up value of N and $G_{\mathrm{CMAF}_f}(z)$ its rounded down value, weighing their contribution through α. Then, after processing (8), the *CMAF's weighted mean value approach* (WCMAF) discrete-time transfer function results in

$$G_{\mathrm{WCMAF}}(z) = \frac{1 - r\, z^{-1}}{1 - z^{-1}}\left[\beta_c\,\frac{1 - z^{-N_c}}{1 - r^{N_c}\, z^{-N_c}} + \beta_f\,\frac{1 - z^{-N_f}}{1 - r^{N_f}\, z^{-N_f}}\right] \qquad (9)$$

where N_c is the rounded value of N up to the nearest integer, N_f is its rounded down value, and β_f and β_c are given by:

$$\beta_c = \frac{\alpha\, k_c}{N_c}, \quad \beta_f = \frac{(1 - \alpha) k_f}{N_f}, \quad \alpha = N - N_f. \qquad (10)$$

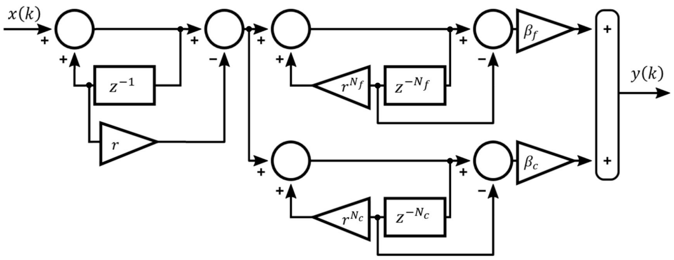

Fig. 2. Block diagram representation of the WCMAF.

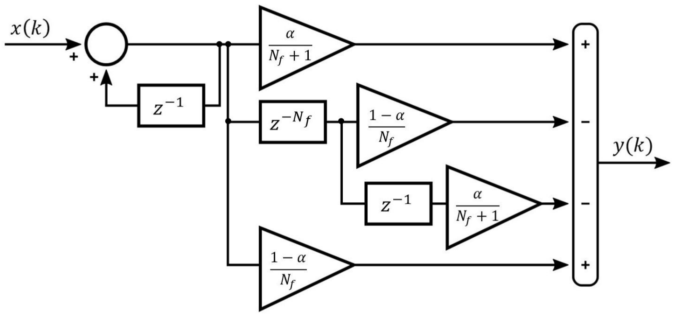

Fig. 3. Block diagram representation of the WMAF.

The constants k_c and k_f are calculated through (7) using N_c or N_f as appropriate. The simplified block diagram representation of the WCMAF is shown in Fig. 2, where $u(k)$ represents the input signal, $t_k = k\,T_s$, $\phi(k)$ is the input signal's phase angle, estimated at the k-th instant, and $M(k)$ its magnitude.

Concerning the *MAF's weighted mean value approach* (WMAF), used for the traditional FF and CF, its discrete-time transfer function is given by

$$G_{\text{WMAF}}(z) = (1-\alpha)G_{\text{MAF}_f}(z) + \alpha\, G_{\text{MAF}_c}(z) \qquad (11)$$

or alternatively

$$G_{\text{WMAF}}(z) = \frac{\frac{1-\alpha}{N_f} - \frac{1-\alpha}{N_f}\, z^{-N_f} + \frac{\alpha}{N_f+1} - \frac{\alpha}{N_f+1}\, z^{-(N_f+1)}}{1-z^{-1}} \qquad (12)$$

where α is also calculated through (10) and its simplified block diagram representation is depicted in Fig. 3.

III. TEST PROTOCOL

Three aspects are sought to be reviewed with this proposal:

1) Tune the attenuation factor r of the phase-lead compensator.
2) Verify that the proposed FF with the WCMAF can still deal with harmonics.
3) Verify that the proposal can provide a faster response than an FF with a non-compensated MAF.

Concerning the tuning of r, a previous testing stage can be done using the IEEE C37.118.1 dynamic compliance during step changes in phase and magnitude. The purpose is to find the value of r that meets the overshoot and response time requirements.

The last two aspects can use the IEEE C37.118.1 standard's steady state compliance and dynamic compliance during step changes in phase and magnitude [6]. The metrics to evaluate are the delay time, response time, and the *total vector error* (TVE), given by

$$\text{TVE}(n) = \sqrt{\frac{\left(\hat{X}_r(n) - X_r(n)\right)^2 + \left(\hat{X}_i(n) - X_i(n)\right)^2}{(X_r(n))^2 + (X_i(n))^2}} \qquad (13)$$

where $\hat{X}_r(n)$ and $\hat{X}_i(n)$ represent the real and imaginary components of the estimated synchrophasor, while $X_r(n)$ and $X_i(n)$ represent the real and imaginary components of the actual phasor. The delay time is the time between a step change is applied to the phasor's amplitude or phase angle and the instant when the stepped parameter reaches 50% of the final steady-state value. The response time is the time it takes for the estimated phasor to reach and hold TVE ≤ 0.01.

As mentioned, the FF with the WCMAF was compared to the FF and the CF, both using the WMAF. The cutoff frequency f_c was set to 60 Hz. Every simulation was performed with the help of Simulink, using $T_s = 10$ kHz as most of the cited works.

The IEEE standard contemplates two phasor estimator performance classes, M class and P class. The P class was chosen for the standard's tests because it is intended for applications that require a fast response, such as in protection systems.

A. Harmonics test

According to [6], the steady-state compliance establishes that the phasor estimator must be tested with an input signal contaminated with one harmonic whose amplitude is equal to 1% of the fundamental signal's amplitude. This must be done for each harmonic up to the 50-th and the steady-state TVE must remain below 1%.

B. Amplitude and phase angle step changes

In this test, a step change will be applied to a three-phase system's signals, and the phasor estimator should provide the positive sequence information. The step changes in magnitude and phase can be mathematically represented as [6]:

$$\begin{aligned} X_a =& X_m\,[1 + k_x\, f_1(t)]\cos(\omega_0\, t + k_a\, f_1(t)),\\ X_b =& X_m\,[1 + k_x\, f_1(t)]\cos(\omega_0\, t - 2\pi/3 + k_a\, f_1(t)),\\ X_c =& X_m\,[1 + k_x\, f_1(t)]\cos(\omega_0\, t + 2\pi/3 + k_a\, f_1(t)). \end{aligned} \qquad (14)$$

Being X_m the amplitude of the input signal, ω_0 the nominal frequency, $f_1(t)$ the unit step function, k_x is the amplitude step size and k_a the phase step size. Then, the positive sequence signal X_1 can be determined as [16, p. 430]:

$$X_1 = \frac{1}{3}\left(X_a + a\,X_b + a^2\,X_c\right) \qquad (15)$$

where $a = -1/2 + \text{j}\sqrt{3}/2 = 1\angle 120°$. The phasor performance requirements are presented in Table I.

C. Case study

As a case study, the IEEE 13 node test feeder [17], [18] was used to test the proposed phasor estimator and compare its response with the FF and CF. The phasor estimator was located at bus 692, and a single-phase to ground fault was

TABLE I
PERFORMANCE REQUIREMENTS UNDER INPUT STEP CHANGE.

Step change specification	Reference condition	Response time	Max overshoot/ undershoot
Magnitude = $\pm 10\%$, $k_x = \pm 0.1$, $k_a = 0$	All test conditions nominal at start or end of step	$1.7/f_0$	5% of step magnitude
Angle = $\pm 10°$, $k_x = 0$, $k_a = \pm\pi/18$	All test conditions nominal at start or end of step	$1.7/f_0$	5% of step magnitude

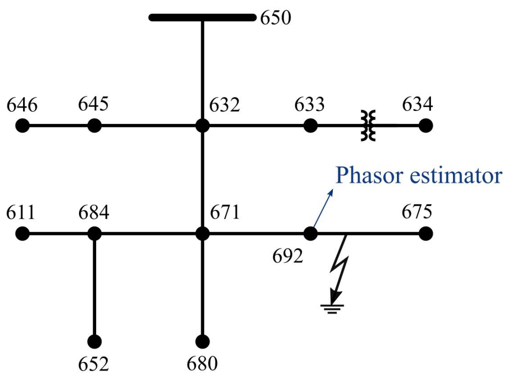

Fig. 4. IEEE 13 node test feeder one line diagram.

simulated at the beginning of line 692-675, next to bus 692—see Fig. 4. This particular type of fault was chosen because it is the most common according to [19, p. 33] and its location was chosen to take advantage of the breaker already present in the simulation model.

The positive sequence signal was measured. Since the fault in question is unsymmetrical, it would be expected that the phasor estimator will record a variation in its amplitude and phase angle.

IV. RESULTS

A. Attenuation factor tuning

Initial tests of the proposed phasor estimator were made using the amplitude $+0.1$ p.u. and phase angle $+10°$ step change tests. The three values of r suggested in [15] were used, being $r = 0.95$, $r = 0.97$, $r = 0.99$ and the results obtained are shown in Table II. It is observed that the closer

TABLE II
PERFORMANCE OF THE PROPOSED PHASOR ESTIMATOR FOR DIFFERENT VALUES OF r.

	Amplitude step change of $+0.1$ p.u.		
	Response time (s)	Delay time (s)	Overshoot (%)
r = 0.95	0.012836	0.0063349	10.9794
r = 0.97	0.016611	0.0050523	18.2581
r = 0.99	0.016679	0.00025383	29.22
	Phase angle step change of $10°$		
	Response time (s)	Delay time (s)	Overshoot (%)
r = 0.95	0.016624	0.0063349	10.9042
r = 0.97	0.016655	0.0050523	18.1093
r = 0.99	0.020893	0.00025383	28.9188

TABLE III
PERFORMANCE OF THE PHASOR ESTIMATOR WITH $r = 0.89$.

	Amplitude step change		
	Response time (s)	Delay time (s)	Overshoot (%)
r = 0.89	0.013924	0.0074242	4.4554
	Phase angle step change		
	Response time (s)	Delay time (s)	Overshoot (%)
r = 0.89	0.014801	0.0074242	4.4297

TABLE IV
COMPARATIVE RESULTS DURING THE HARMONICS TESTS.

	FF TVE (%)	CF TVE (%)	r = 0.89 TVE (%)
Maximum	0.0077518	1.2643	0.043331
Minimum	0.005177	1.2615	0.0061685
Average	0.0064389	1.2630	0.0196956

r is to unity, the lower the phase delay, which is reflected in the standardized measure of the delay time. The shortest delay time was 253.83 µs, achieved with $r = 0.99$. Concerning the response time, the IEEE standard establishes that it shall not be greater than $1.7/f_0 \approx 0.0283$ s, which is met with any of the three r values. In this case, the shortest response times were achieved with $r = 0.95$.

However, it can be observed in Table II that non of the three values of r met the 5% overshoot requirement. It was needed a value of $r = 0.89$ to fulfill the standard. The latter appears to indicate that only values below 0.90 can comply with the IEEE standard. Table III summarizes the results under the same amplitude and phase angle step changes of $+0.1$ p.u. and $+10°$. This version showed an even lower response time than with $r = 0.95$. In consequence, it can be inferred that a reduction in r implies a reduction in the response time.

B. Harmonics test

It was observed that the FF, CF, and FF with the WCMAF attained the minimum TVE at the 2nd harmonic and the maximum at the 50th. This error is associated with T_s because the 50th harmonic cannot be effectively represented with such bandwidth. In this sense, only signals below 2.5 kHz are adequately represented due to sampling. The results are summarized in Table IV, it can be seen that only the FF and the WCMAF-FF met the IEEE standard, being the FF the one that showed the lowest TVE values.

The percentage difference between the average TVE of the WCMAF-FF and the FF is 0.01326%. Therefore, the WCMAF-FF showed a slight, insignificant increase in the TVE, confirming that the compensator does not degrade the MAF's harmonic rejection.

C. Amplitude and phase angle step changes

The results after amplitude step changes of $+0.1$ p.u. and -0.1 p.u. are shown in Table V. Similarly, Table VI shows the results under phase angle step changes of $10°$ and $-10°$. Both tables include the WCMAF-FF results with $r = 0.99$ for the sake of comparison. Without considering $r = 0.99$, the proposed phasor estimator with $r = 0.89$ showed the shortest response times and delay times in all the tests. However, the

TABLE V

COMPARATIVE RESULTS UNDER THE AMPLITUDE STEP CHANGES.

Step change of +0.1 p.u.			
	Response time (s)	Delay time (s)	Overshoot (%)
FF	0.014733	0.0081333	2.37590E-11
CF	0.018732	0.0093594	0.03432
r = 0.89	0.013924	0.0074242	4.4554
r = 0.99	0.016679	0.0002538	29.22
Step change of −0.1 p.u.			
	Response time (s)	Delay time (s)	Undershoot (%)
FF	0.015067	0.0081333	1.72080E-11
CF	0.017251	0.0093646	0.06361
r = 0.89	0.014257	0.0074242	4.4554
r = 0.99	0.017078	0.0002538	29.22

TABLE VI

COMPARATIVE RESULTS UNDER THE PHASE ANGLE STEP CHANGES.

Step change of 10°			
	Response time (s)	Delay time (s)	Overshoot (%)
FF	0.01561	0.0081333	3.67160E-10
CF	0.019112	0.0097468	3.5708
r = 0.89	0.014801	0.0074242	4.4297
r = 0.99	0.020893	0.0002538	28.9188
Step change of −10°			
	Response time (s)	Delay time (s)	Undershoot (%)
FF	0.01561	0.0081333	1.86450E-10
CF	0.018197	0.0090254	3.6292
r = 0.89	0.014801	0.0074242	4.4297
r = 0.99	0.020893	0.0002538	28.9188

FF had the lowest overshoots and undershoots. In Table VII, the average percentage changes in delay and response times between the WCMAF-FF and the FF are presented. Using $r = 0.89$, it is observed an average reduction in delay time of 8.72% as well as a 5.31% response time reduction. On the other hand, with $r = 0.99$, the delay time was reduced by 96.88%, and the response time increased by 41.81%.

Hence, from this test it follows that the WCMAF-FF with $r = 0.89$ did meet the standard and show a faster transient response than the FF and CF, but it was not a significant improvement. On the other hand, the estimator with $r = 0.99$ does show a significant improvement, but the problem is that this version does not meet the standard.

D. IEEE 13 node feeder case study

Fig. 6 and Fig. 5 show the current and voltage estimated phasors, respectively, during the simulation of the phase to ground fault in the IEEE 13 node test feeder. Both graphs confirm that the WCMAF-FF-based phasor estimator was the one that provided the fastest transient response compared to the FF and the CF. However, concerning the $r = 0.89$ version, the improvement is indeed insignificant and the response is very similar to that of the FF. For the $r = 0.99$ version, its transient response did show a significant improvement but also a significant increase in the overshoots/undershoots. On the other hand, notice that the CF fails in estimating the phase angle, mostly due to the fixed discrete delay shown in (2).

TABLE VII

AVERAGE PERCENTAGE CHANGES IN DELAY AND RESPONSE TIMES

	Delay Time (%)	Response Time (%)
r = 0.89	-8.72	-5.31
r = 0.99	-96.88	41.81

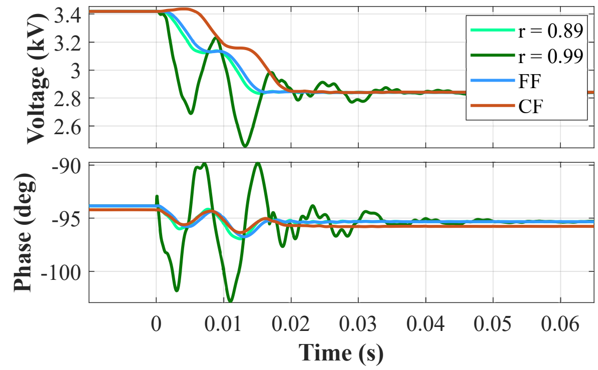

Fig. 5. Voltage's amplitude and phase angle results from the case study.

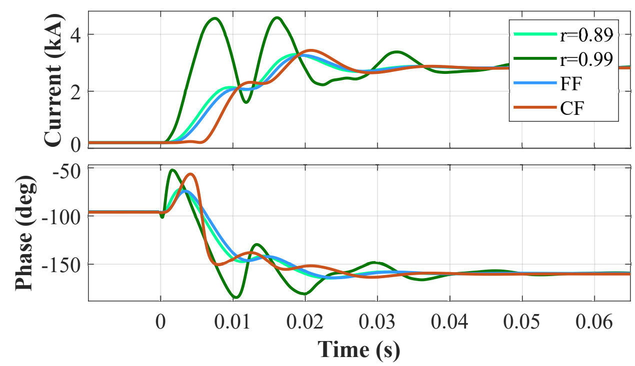

Fig. 6. Current's amplitude and phase angle results from the case study.

V. CONCLUSION

In this paper, an FF-based phasor estimator with a MAF and a phase-lead compensator was proposed to solve the problem of the MAF's phase delay. The proposed estimator exhibited a faster transient response while preserving its ability to eliminate harmonics. It was observed that the attenuation factor must be $r < 0.9$ to meet the 5% overshoot/undershoot required by the IEEE synchrophasors standard, and that reducing r also reduces the overshoot and response time, but increases the delay. Although the WCMAF-FF with $r = 0.89$ met the standard and showed a faster transient response than the FF and CF, it did not significantly reduce the delay time with respect to the FF. On the other hand, the WCMAF-FF with $r = 0.99$ did significantly reduce the delay time, but this version did not meet the standard. Perhaps, if this estimator were intended to be used for protection systems applications, such as fault detection, it would be convenient to use it with $r = 0.99$; however, this decision will be up to the system's designer. For future work, it would be worthwhile to pay special attention to decreasing the overshoot/undershoot of the WCMAF-FF with high values of r.

REFERENCES

[1] S. A. Aleem, A. Y. Abdelaziz, A. F. Zobaa, and R. Bansal, *Decision Making Applications in Modern Power Systems*. Academic Press, Sep. 2019, google-Books-ID: owaxDwAAQBAJ.

[2] V. C. Gungor, B. Lu, and G. P. Hancke, "Opportunities and Challenges of Wireless Sensor Networks in Smart Grid," *IEEE Transactions on Industrial Electronics*, vol. 57, no. 10, pp. 3557–3564, Oct. 2010, conference Name: IEEE Transactions on Industrial Electronics.

[3] M. Q. Khan, M. M. Ahmed, A. M. A. Haidar, N. Julai, and M. K. Hasan, "Synchrophasors Based Wide Area Protection and Phasor Estimation: A Review," in *2018 IEEE 7th International Conference on Power and Energy (PECon)*, Dec. 2018, pp. 215–220.

[4] J. D. L. Ree, V. Centeno, J. S. Thorp, and A. G. Phadke, "Synchronized Phasor Measurement Applications in Power Systems," *IEEE Transactions on Smart Grid*, vol. 1, no. 1, pp. 20–27, Jun. 2010, conference Name: IEEE Transactions on Smart Grid.

[5] I. F. Akyildiz, Weilian Su, Y. Sankarasubramaniam, and E. Cayirci, "A survey on sensor networks," *IEEE Communications Magazine*, vol. 40, no. 8, pp. 102–114, Aug. 2002, conference Name: IEEE Communications Magazine.

[6] IEEE Power & Energy Society, "IEEE Standard for Synchrophasor Measurements for Power Systems," *IEEE Std C37.118.1-2011 (Revision of IEEE Std C37.118-2005)*, pp. 1–61, Dec. 2011, conference Name: IEEE Std C37.118.1-2011 (Revision of IEEE Std C37.118-2005).

[7] J. A. de la O Serna, "Synchrophasor Measurement With Polynomial Phase-Locked-Loop Taylor–Fourier Filters," *IEEE Transactions on Instrumentation and Measurement*, vol. 64, no. 2, pp. 328–337, Feb. 2015, conference Name: IEEE Transactions on Instrumentation and Measurement.

[8] F. Messina, P. Marchi, L. Rey Vega, C. G. Galarza, and H. Laiz, "A Novel Modular Positive-Sequence Synchrophasor Estimation Algorithm for PMUs," *IEEE Transactions on Instrumentation and Measurement*, vol. 66, no. 6, pp. 1164–1175, Jun. 2017, conference Name: IEEE Transactions on Instrumentation and Measurement.

[9] O. Chaari, M. Meunier, and F. Brouaye, "Wavelets: a new tool for the resonant grounded power distribution systems relaying," *IEEE Transactions on Power Delivery*, vol. 11, no. 3, pp. 1301–1308, Jul. 1996, conference Name: IEEE Transactions on Power Delivery.

[10] A. Rahmati, R. Adhami, and M. Dimassi, "Real-time electrical variables estimation based on recursive wavelet transform," *International Journal of Electrical Power & Energy Systems*, vol. 68, pp. 170–179, Jun. 2015. [Online]. Available: https://www.sciencedirect.com/science/article/pii/S0142061514007789

[11] K. Chauhan, M. V. Reddy, and R. Sodhi, "A Novel Distribution-Level Phasor Estimation Algorithm Using Empirical Wavelet Transform," *IEEE Transactions on Industrial Electronics*, vol. 65, no. 10, pp. 7984–7995, Oct. 2018, conference Name: IEEE Transactions on Industrial Electronics.

[12] J. A. de la O Serna and J. Rodríguez-Maldonado, "Taylor–Kalman–Fourier Filters for Instantaneous Oscillating Phasor and Harmonic Estimates," *IEEE Transactions on Instrumentation and Measurement*, vol. 61, no. 4, pp. 941–951, Apr. 2012, conference Name: IEEE Transactions on Instrumentation and Measurement.

[13] C. Huang, X. Xie, and H. Jiang, "Dynamic Phasor Estimation Through DSTKF Under Transient Conditions," *IEEE Transactions on Instrumentation and Measurement*, vol. 66, no. 11, pp. 2929–2936, Nov. 2017, conference Name: IEEE Transactions on Instrumentation and Measurement.

[14] S. Golestan, M. Ramezani, J. M. Guerrero, F. D. Freijedo, and M. Monfared, "Moving Average Filter Based Phase-Locked Loops: Performance Analysis and Design Guidelines," *IEEE Transactions on Power Electronics*, vol. 29, no. 6, pp. 2750–2763, Jun. 2014, conference Name: IEEE Transactions on Power Electronics.

[15] S. Golestan, J. M. Guerrero, and A. M. Abusorrah, "MAF-PLL With Phase-Lead Compensator," *IEEE Transactions on Industrial Electronics*, vol. 62, no. 6, pp. 3691–3695, Jun. 2015, conference Name: IEEE Transactions on Industrial Electronics.

[16] J. D. Glover, M. S. Sarma, and T. Overbye, *Power System Analysis & Design, SI Version*. Cengage Learning, Aug. 2012, google-Books-ID: HrtXToLEbVoC.

[17] W. Kersting, "Radial distribution test feeders," in *2001 IEEE Power Engineering Society Winter Meeting. Conference Proceedings (Cat. No.01CH37194)*, vol. 2, Jan. 2001, pp. 908–912 vol.2.

[18] MathWorks, "IEEE 13 Node Test Feeder - MATLAB & Simulink - MathWorks América Latina." [Online]. Available: https://la.mathworks.com/help/physmod/sps/ug/ieee-13-node-test-feeder.html

[19] M. V. Titarenko and I. Noskov-Dukel'skii, *Protective Relaying in Electric Power Systems*. Peace Publishers, 1963, google-Books-ID: QwFe9muPr6sC.